Electric dipoles in rare-earth-doped SrF_2. Relaxation parameters and dipole-dipole interaction

W. van Weperen and H. W. den Hartog
Solid State Physics Laboratory, 1 Melkweg, Groningen, The Netherlands
(Received 10 February 1978)

Ionic crystals of SrF_2 doped with trivalent rare-earth ions have been investigated by means of the ionic thermocurrent (ITC) technique. The experimentally obtained ITC curves have been fitted by a refined ITC formula, giving values for the relaxation parameters E_0 and τ_0, and, additionally, for the broadening parameter p, which accounts for the interaction between dipoles. This interaction may come about either by electrostatic interaction between dipoles, or by elastic deformation of the lattice caused by distant dipolar defects. Both effects are considered theoretically. From a comparison with the experimental results we infer that each one of them contributes significantly to the broadening of the ITC bands. A consistent picture has been obtained with regard to the relaxation parameters E_0 and τ_0. For type-I dipoles in SrF_2:R^{3+} we have found that $E_0 = 0.47 \pm 0.02$ eV and type-II dipoles give $E_0 = 0.64 \pm 0.01$ eV; τ_0 appears to be almost independent of the nature of the R^{3+} ion. SrF_2:Sm and SrF_2:Eu show a deviating behavior, which is explained by assuming the presence of divalent Sm and Eu ions in the sample.

I. INTRODUCTION

One of the most elegant methods for determination of the relaxation parameters of electric dipoles in ionic crystals is the ionic thermocurrent (ITC) technique, introduced a good ten years ago by Bucci and Fieschi.[1] Several authors since have published results of ITC experiments on alkaline-earth halides doped with low concentrations of trivalent rare-earth ions.

The excess charge of the rare-earth ion is compensated locally by an interstitial halide ion at a nearest-neighbor (nn) position, giving rise to type-I dipoles, or at a next-nearest-neighbor (nnn) position, giving type-II dipoles, as shown in Fig. 1 for SrF_2. The available data for type-I dipoles in CaF_2:R^{3+} show a rather large scatter in the relaxation parameters E and τ_0, the activation energy

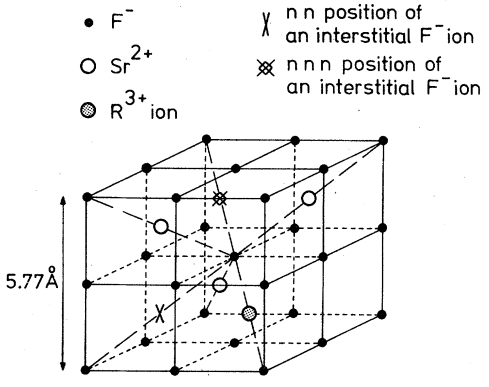

FIG. 1. Three-dimensional schematic representation of a SrF_2 crystal showing the structure of type-I and type-II dipoles.

for reorientation and the characteristic relaxation time, respectively. For example, Kitts and Crawford[2] find $E = 0.420$ eV, $\tau_0 = 2.5 \times 10^{-15}$ sec, and Stiefbold and Huggins[3] report $E = 0.510$ eV, $\tau_0 = 1.4 \times 10^{-16}$ sec for CaF_2:Gd^{3+}.

In a previous publication by our group[4] it was shown that E and τ_0 are strongly correlated, and depend on the concentration of dipoles. It was suggested that dipole-dipole interactions can explain the observed features like broadening of the ITC curve and concentration dependence of E and τ_0. Recently, we have worked this out[5] by assuming a Gaussian distribution of activation energies which spreads symmetrically about the unperturbed energy E_0. This leads to an extra parameter p in the ITC formula, which is a measure for the width of the energy distribution. ITC curves from samples of SrF_2, doped with varying concentrations of Ce, have been analyzed with the refined ITC formula, giving E_0 and τ_0 independent of the dipole concentration, and a linear relation between p and the dipole concentration.

For low dopant concentration the ITC curve can be successfully described by the well-known expression

$$I(T) = \frac{C}{\tau_0} e^{-E/kT} \exp\left(-\int_0^T \frac{f'(T')}{\tau_0} e^{-E/kT'} dT'\right), \tag{1}$$

where

$$C = A(N_d \mu_e^2 V/3dkT_{p,\mathrm{eff}})\Pi, \tag{2}$$

with

$$\Pi = 1 - \exp[-t_p/\tau(T_p)]. \tag{3}$$

For the meaning of the various symbols we refer

to previous papers.[4,5] This expression, however, cannot successfully explain the experimental curves obtained from moderately and heavily doped samples. When dipole-dipole interaction is taken into account by introducing the extra parameter p, the quality of the fitted curve becomes comparable with that of a low-concentration curve analyzed with formula (1). The extended ITC formula thus leads to a highly improved reliability of the obtained values of the relaxation parameters (E_0 and τ_0).

In this paper we present the results of ITC experiments on $SrF_2:R^{3+}$, where R stands for the rare earths La, Ce, Pr, Nd, Sm, Eu, Gd, Tb, Dy, Ho, Er, Tm, Yb, and Lu. Lenting *et al.*[4] observed low-temperature peaks in SrF_2:La–Dy, with the temperature of the maximum current $T_m \approx 150$ K, and higher-temperature peaks in SrF_2:Gd–Lu with $T_m \approx 210$ K. The low-temperature peaks were ascribed to type-I dipoles and the high-temperature peaks to type-II dipoles. These assignments have by and large been confirmed by the results of the analyses with the refined ITC formula. A deviating behavior is observed only for SrF_2:Sm and SrF_2:Eu. For these elements we believe type-II instead of type-I compensation to occur in SrF_2 with $T_m \approx 150$ K.

Infrared experiments performed by Timans and den Hartog[6] on R^{3+}-H_i^- dipoles in SrF_2 indicate that τ_0 is almost independent of the nature of the R^{3+} ion. Our results suggest the same for R^{3+}-F_i^- complexes in SrF_2.

Furthermore, we present some tentative conclusions on the reorientation mechanism of the dipoles. It is suggested that, next to electrostatic dipole-dipole interaction, also elastic deformations contribute to the broadening of the ITC bands.

II. THEORY

A. ITC formula

We have shown[5] that the ITC formula, extended to take dipole-dipole interaction into account, can be written

$$I(T) = I^*(T) F(E_0, \tau_0, p, T), \tag{4}$$

where $I^*(T)$ has the form of the original ITC formula (1) with $E = E_0$ and F is a correction factor containing the width p of the energy distribution. The expression for F given earlier[5] requires excessive computing times for the curve fitting process, as it contains an integral that can only be evaluated numerically.

It is possible however to reduce the necessary computing times by a factor of about 10 when an additional approximation is made (cf. Ref. 5):

$$F \simeq \frac{1}{p\sqrt{\pi}} \int_{-\infty}^{+\infty} dE \, \exp\left[-\frac{E-E_0}{kT} - \left(\frac{E-E_0}{p}\right)^2 - \frac{aT}{\tau_0}\left(\frac{e^{-E/kT}}{E/kT+2} - \frac{e^{-E_0/kT}}{E_0/kT+2}\right)\right] . \tag{5}$$

a is the reciprocal heating rate at $T = T_m$. It is allowed to take $-\infty$ as the lower boundary of the interval of integration instead of 0, which is physically correct, because of the almost disappearing contribution to F of the extra interval. With the substitution $(E - E_0)/p = x$, Eq. (5) becomes

$$F \simeq \frac{1}{\sqrt{\pi}} \int_{-\infty}^{+\infty} dx e^{-x^2} g(x) \simeq \frac{1}{\sqrt{\pi}} \sum_{i=1}^{n} w_i g(x_i) . \tag{6}$$

The last transition follows from the theory of functions (cf. Abramowitz and Stegun[7]) which also gives the values of the weight factors w_i. The x_i are the zeroes of the nth-degree Hermite polynomial. In practical ITC applications it is sufficient to take $n = 20$ in order to achieve an accuracy better than 1 in 10^6 for the approximation in Eq. (6).

B. Dipole-dipole interaction

The interaction energy of two dipoles $\vec{\mu}_1$ and $\vec{\mu}_2$ with a distance $\vec{r}_{12}$ between them, is given by

$$U = \frac{1}{4\pi\epsilon\epsilon_0}\left(\frac{\vec{\mu}_1 \cdot \vec{\mu}_2}{r_{12}^3} - \frac{3(\vec{\mu}_1 \cdot \vec{r}_{12})(\vec{\mu}_2 \cdot \vec{r}_{12})}{r_{12}^5}\right) , \tag{7}$$

where ϵ is the static dielectric constant of the medium in which the dipoles are embedded. When P is the dipole moment *in vacuo*, we write for the effective moment of a dipole in SrF_2 ($\epsilon = 7.69$), $\mu = [3\epsilon/(2\epsilon+1)]P = 1.41P$ (cf. Böttcher[8]).

In our last paper[5] we presented a rather crude model that allows one to predict theoretically the order of magnitude of the broadening parameter p. In this model the reorienting dipole $\vec{\mu}_1$ is placed at the center of a sphere with a radius such that the sphere contains only one additional dipole $\vec{\mu}_2$. $\vec{\mu}_2$ is assumed to be randomly oriented, as one can easily show that the average dipole moment $\bar{\mu} \ll \mu$.

The dipoles are taken to be point dipoles, situated at the R^{3+} positions. Furthermore, we assume that there is a random distribution of $\vec{\mu}_2$ over all Sr^{2+} lattice sites within the sphere, and we only consider the perturbation of $\vec{\mu}_1$ that is caused by $\vec{\mu}_2$. From the values of the interaction energy as given by Eq. (7), calculated for all possible positions and directions of $\vec{\mu}_2$, a histogram of $N(U)$ can be constructed. The theoretical value for p follows from the fit of a Gaussian distribution to the histogram. In our last paper[5] we only considered the perturbation of $\vec{\mu}_1$ in its equilibrium position. For nn dipoles this model can be refined when one assumes the length of $\vec{\mu}_1$ during reorientation to remain constant. This is not exactly the case for the isolated R^{3+}-F_i^- complex, because also some surrounding F^- ions are temporarily displaced by the jumping F_i^- ion. The overall dipole strength in the saddle-point configuration, corresponding with maximum potential energy of the reorienting dipole, will then approximately equal its equilibrium strength.

Now, if we further assume that the saddle point lies halfway between two equilibrium positions, the energy difference between bottom and top of the potential barrier, as caused by $\vec{\mu}_2$ can be calculated. Again a histogram can be generated and p, according to the refined model, obtained.

For nnn dipoles it is more difficult to make reasonable suppositions about the dipole moment during reorientation and the location of the saddle point. We therefore only applied the crude model to these dipoles. In both the crude and the refined model p increases linearly with the dipole concentration N_d. Table I gives the slopes m from $p = mN_d$. It is seen that the improved model leads to values of p that are only little less than those arising from the crude model: the difference is 8%.

In view of Eq. (7) one would expect at first sight for the ratio of m_b and m_a (crude model applied to nnn and nn dipoles, respectively): $m_b/m_a = (\mu_{nnn}/\mu_{nn})^2 = 3$. It appears that $m_b/m_a = 3.73$. This means that besides the dipole strengths, also the various possible orientations of the dipoles with respect to each other, determine the width of the energy distribution.

TABLE I. Theoretical calculation of m in $p = mN_d$. Only electrostatic interaction between dipoles has been considered. The models have been explained in the text.

Model	Interacting dipoles	m (10^{-18} eV cm^3)
Crude	Type I	$m_a = 0.000131$
Crude	Type II	$m_b = 0.000488$
Refined	Type I	$m_c = 0.000121$

In addition to electrostatic dipole-dipole interaction, also elastic deformations due to the presence of perturbing dipoles may give rise to a broadening of the ITC band. The fact that the jump energy for a free interstitial fluorine ion (0.94 eV in SrF_2) is different from the reorientation energy of an F_i^- ion that is part of an R^{3+}-F_i^- dipole complex is due to elastic deformation of the lattice by the R^{3+} ion.

We write for the change in the activation energy of the F_i^- ion

$$\Delta E = -\alpha/r^n . \tag{8}$$

In Sec. III we show that the reorientation energies of nn dipoles ($r = 2.9$ Å) and nnn dipoles ($r = 5.0$ Å) are 0.47 and 0.64 eV, respectively. It follows that $n \approx 1$ and $\alpha \approx 1.3$ eV Å. Equation (8) accounts for the contribution to the broadening of activation energies from elastic deformations caused by the presence of the R^{3+} monopole. Here we are interested in the effect of a dipole on the reorientation energy of an F_i^- ion at a distance $\vec{r}$ from the dipole. The energy shift is given by

$$\Delta E_d = (\alpha/r^3)\vec{r}\cdot\vec{d}\,, \tag{9}$$

where $\vec{d}$ is the vector connecting the components of the perturbing dipole.

In order to find out whether elastic deformations contribute significantly to the line broadening of an ITC curve, Eq. (9) should be compared with Eq. (7), which gives the effect of electrostatic interaction. The ratio η of the two types of interaction effects equals

$$\eta = |\Delta E_d/U| \approx (4\pi\epsilon\epsilon_0\alpha d/\mu^2)r = 0.12r \tag{10}$$

(r in angstrom units) for nn dipoles in SrF_2.

In practice, typical distances between dipoles range from 10 to 50 Å, approximately. Consequently, elastic effects may be comparable in magnitude with electrostatic interaction. The above derivation is far from exact and gives only a rough estimate of the relative contributions of the two effects. For example, η contains μ, the value of which is not known accurately.

When electrostatic interactions are taken into account only, the relation between p and the dipole concentration N_d is exactly linear. The elastic interaction effect falls off with the distance slower and gives rise to a linear relation between p and $N_d^{2/3}$. The range of observed dipole concentrations is not sufficient to decide which of the two effects is dominant.

C. Interaction between different kinds of dipoles

When two different kinds of dipoles, $\vec{\mu}_1$ and $\vec{\mu}_2$ are present in one sample, e.g., SrF_2:Gd, the

broadening p_1 of the ITC band as measured from the reorientation of $\vec{\mu}_1$ dipoles consists of two contributions. The first (p_{11}) is caused by the interaction between identical dipoles ($\vec{\mu}_1$), the second one (p_{12}) arises from the interaction between different dipoles ($\vec{\mu}_1$ and $\vec{\mu}_2$).

If we assume that the interaction is entirely electrostatic, i.e., if it is described by Eq. (7), a relation can be derived for the ratio of the actual dipole strengths that does not contain the dipole concentrations N_1 and N_2. This is important because ITC experiments only yield values for the product $\mu^2 N$; we are not able to separate the unknown parameters μ and N.

From Sec. II B we infer that the width of the energy distribution can be written

$$p = \gamma p_0 \mu^2 N = mN , \tag{11}$$

where γ is a geometrical factor, p_0 a proportionality constant, μ the effective dipole moment, and N the dipole concentration. It follows that $p_{11} = \gamma_{11} p_0 \mu_1^2 N_1$ and $p_{12} = \gamma_{12} p_0 \mu_1 \mu_2 N_2$. As the energy distributions are Gaussian, the widths should be summed quadratically:

$$p_1^2 = p_{11}^2 + p_{12}^2 = (p_0 \mu_1)^2 [(\gamma_{11} \mu_1 N_1)^2 + (\gamma_{12} \mu_2 N_2)^2] .$$

Analogously, we write for the broadening of the second peak

$$p_2^2 = (p_0 \mu_2)^2 [(\gamma_{21} \mu_1 N_1)^2 + (\gamma_{22} \mu_2 N_2)^2] .$$

In Sec. II B we have shown theoretically on the basis of the crude model that $\gamma_{22}/\gamma_{11} = 3.73/3 = 1.24$. For the refined model we expect the influence of the geometrical factors to decrease. Then, with the approximation $\gamma_{11} = \gamma_{12} = \gamma_{21} = \gamma_{22}$, it follows that

$$p_2/p_1 = \mu_2/\mu_1 . \tag{12}$$

If the two kinds of dipoles are studied separately, i.e., in different samples, one obtains from Eq. (11) values for m_1 and m_2. Their ratio is given approximately by

$$m_2/m_1 = (\mu_2/\mu_1)^2 . \tag{13}$$

The experimental values of m_1 and m_2 are in fact calculated from undistorted-point-ion model (UPIM) values for the dipole moments μ_1 and μ_2. This seemingly interferes with the usefulness of Eq. (13). Nevertheless, it can be seen that identical amplification factors, e.g., $3\epsilon/(2\epsilon+1)$,[4] necessary to account for the surrounding dielectric, leave the ratio m_2/m_1 unaffected.

It should be noted that Eqs. (11)–(13) only hold when elastic perturbations [see Eq. (9)] are negligible with respect to electrostatic interactions. In the opposite case, i.e., when the interaction is governed by Eq. (9), Eq. (11) should be replaced by

$$p = \gamma' p_0' \mu N^{2/3} = m' N^{2/3} . \tag{14}$$

When two kinds of dipoles are present in one sample, it follows for the ratio of the respective broadening parameters:

$$p_2/p_1 = 1 . \tag{15}$$

When the different dipoles are studied in different samples, we find instead of Eq. (13),

$$m_2/m_1 \approx m_2'/m_1' = \mu_2/\mu_1 . \tag{16}$$

A confrontation of Eqs. (12) and (13) and their counterparts (15) and (16) with the experimental results may lead to a conclusion about the relative magnitudes of the two types of interaction.

III. EXPERIMENTAL RESULTS

The experimental procedure does not differ from the one described in our previous papers.[4,5]

A. Type-I dipoles in $SrF_2 : R^{3+}$

In SrF_2:La, Ce, Pr, Nd, Sm, Eu, Gd, Tb, Dy we observed ITC peaks with $T_m \approx 150$ K. Sm and Eu show some remarkable features, which will be discussed in Sec. III C. The results obtained from the remaining rare earths have been compiled in Table II. The values for SrF_2:Ce, taken from a

TABLE II. ITC data for type-I dipoles in $SrF_2:R^{3+}$. The results of SrF_2:Ce have been published before (Ref. 5).

Dopant	E_0 (eV)	p (eV)	τ_0 (sec)	N_d (cm^{-3})	T_m (K)
La	0.471	0.0011	3.1×10^{-14}	10×10^{17}	153.5
Ce	0.48 ± 0.01	···	$1\times10^{-14\pm0.3}$	···	151.2 – 152.1
Pr	0.472	0.0039	2.4×10^{-14}	48×10^{17}	152.7
Nd	0.479	0.0031	1.3×10^{-14}	41×10^{17}	152.5
Gd	0.471	0.0004	1.7×10^{-14}	19×10^{17}	151.1
Tb	0.457	0.0042	2.0×10^{-14}	21×10^{17}	147.4
Dy	0.451	0.0047	4.3×10^{-14}	8×10^{17}	148.3

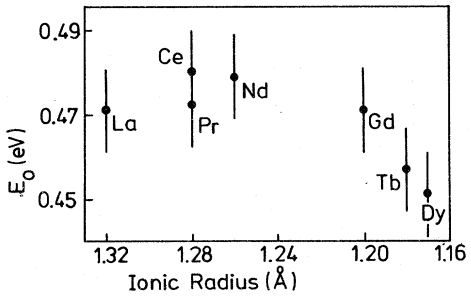

FIG. 2. Variation of E_0 as a function of the R^{3+} radius for type-I dipoles in $SrF_2:R^{3+}$.

series of ten different crystals, have been published before.[5] Figure 2 shows the activation energies as a function of the ionic radius of the impurity ion. The radii were taken from the work of Shannon and Prewitt.[9] Table II shows that there is no significant correlation between τ_0 and the ionic radius of the R^{3+} ion. The maximum error in $\log_{10}\tau_0$ is estimated to amount to 0.5.

The determination of T_m is straightforward and gives accurate values with maximum errors of 1 K. From the behavior of T_m as a function of ionic radius and from the relation

$$E_0/kT_m^2=[f'(T_m)/\tau_0]\exp(-E_0/kT_m)\,, \qquad (17)$$

one can therefore conclude that it is not meaningful to draw a straight line through the experimental points in Fig. 2. From Eq. (17) one can derive that $E_0 \sim T_m$, approximately. The experimental values are seen to agree roughly with this relation.

In Fig. 3 we have plotted p as a function of the dipole concentration for type-I dipoles. The drawn line in this diagram originates from the results of $SrF_2:Ce^{3+}$, published before.[5] The p values of La, Pr, Nd, and Gd confirm the slope of this line. The

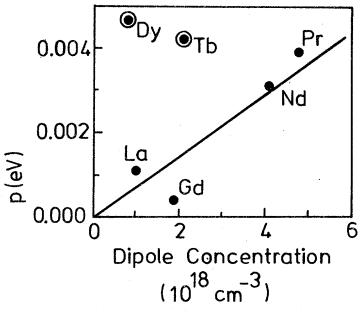

FIG. 3. Behavior of p as a function of the dipole concentration for type-I dipoles in $SrF_2:R^{3+}$. The straight line originates from previous work (Ref. 5). The slope is $m_1 = 0.00074\times10^{-18}$ eV cm^3.

TABLE III. ITC data for type-II dipoles in $SrF_2:R^{3+}$.

Dopant	E_0 (eV)	p (eV)	τ_0 (sec)	N_d (cm^{-3})	T_m (K)
Gd	0.639	0.0000	3.6×10^{-14}	3×10^{17}	206.2
Tb	0.639	0.0081	3.7×10^{-14}	38×10^{17}	206.0
Dy	0.641	0.0060	6.9×10^{-14}	56×10^{17}	210.0
Ho	0.642	0.0083	10.0×10^{-14}	123×10^{17}	212.5
Er	0.644	0.0103	8.9×10^{-14}	81×10^{17}	212.5
Tm	0.640	0.0106	6.4×10^{-14}	66×10^{17}	209.7
Yb	0.650	0.0119	3.2×10^{-14}	84×10^{17}	208.8
Lu	0.631	0.0054	2.3×10^{-14}	55×10^{17}	210.8

relatively large values found for Dy and Tb arise from the appreciable concentrations of type-II dipoles that are also present in these samples. The concentration of type-II dipoles in $SrF_2:Gd^{3+}$ is too small to influence the broadening of the type-I reorientation curve significantly (cf. Table III).

B. Type-II dipoles in $SrF_2:R^{3+}$

Table III gives the results of the observed type-II dipoles. It should be noted that the type-II values given for SrF_2:Dy and those given in Table II were taken from different samples. The results of Gd and Tb in Tables II and III each originate from only one crystal. Figure 4 shows E_0 plotted versus the radius of the R^{3+} ion. Within the experimental errors E_0 follows the variations in T_m, as it does for type-I dipoles. Again the maximum error of 0.5 in $\log_{10}\tau_0$ leaves no room for conclusions about a possible relation between τ_0 and the ionic radius. The average value of τ_0 for type-II dipoles is seen to be slightly higher than the average τ_0 for type-I dipoles.

In Fig. 5 the relation between p and N_d is shown graphically. The straight line represents a least-squares fit to the experimental data; the ones associated with Tb and Gd are excluded, because of the presence of appreciable concentrations of type-I dipoles in the same sample.

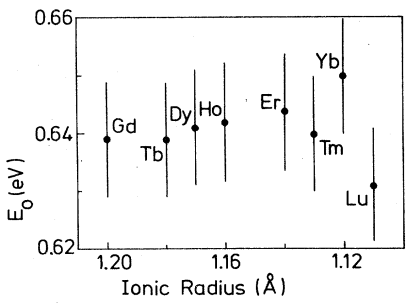

FIG. 4. Variation of E_0 as a function of the R^{3+} radius for type-II dipoles in $SrF_2:R^{3+}$.

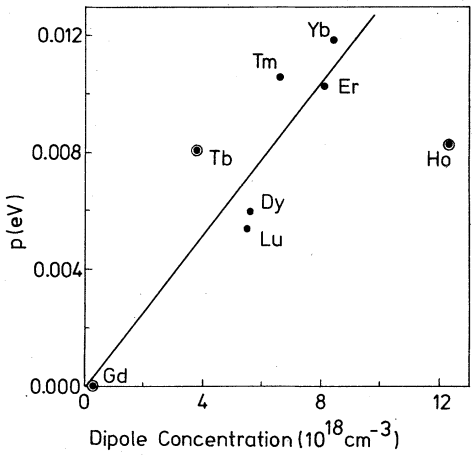

FIG. 5. Behavior of p as a function of the dipole concentration for type-II dipoles in $SrF_2:R^{3+}$. The drawn line represents a least-squares fit to the data of Dy, Er, Tm, Yb, and Lu; the slope is $m_2 = 0.00131 \times 10^{-18}$ eV cm^{-3}.

From the work of Lenting *et al.*[4] we know that the ratios between the numbers of type-I and type-II dipoles in SrF_2:Gd, Tb, Dy are 6.0, 0.5, and 0.07, respectively. Therefore the influence on the broadening of the nnn peak in SrF_2:Dy, as caused by the nn dipoles, may be neglected. The results of SrF_2:Ho have not been included in the calculation of the straight line shown in Fig. 5 either. In this sample a very high dipole concentration, which possibly causes some dipole clustering, has been observed. As a result of dipole-dipole interaction the clustered dipoles are then expected to line up preferentially along a common direction. This correlation reduces the spread in the reorientation energies and thus the observed value of p.

C. SrF_2: Sm and SrF_2: Eu

The ITC spectrum of SrF_2:Sm shows a peak of considerable intensity at $T_m \approx 146$ K (peak a) immediately followed by a very small one with $T_m \approx 161$ K (peak b). Two different samples have been analyzed. We only studied peak a of the first sample, whereas the intensity of peak b has also been observed as a function of the polarization time t_p and the polarization temperature T_p. Table IV summarizes the results. The most plausible inference would be to assign peak a to the reorientation of nn dipoles. Calculation of N_d, however, then leads to a value of 82×10^{17} cm^{-3} for peak $a1$.

When the corresponding p (0.0020 eV) is marked in Fig. 3, it can be seen that it does not correspond with the other type-I dipole data. If we assume peak a to originate from type-II dipoles, then $N_d = 27 \times 10^{17}$ cm^{-3}, which matches remarkably well the picture of type-II dipoles in Fig. 5. In sample 2 an additional unidentified ITC band with comparable intensity near $T_m = 300$ K has been observed, which is responsible for the larger values of p found in this sample.

From Table IV it can also be deduced that the observed variations in $N_d\Pi$ for peaks $a1$ through $a5$ cannot be explained by the respective values of Π that are calculated from t_p, T_p, E_0, and τ_0. One can even conclude from the results of sample 2 that no single combination of E_0 and τ_0 can be found to describe the observations. Additional experiments have shown that the dipole concentration does not depend on the time elapsed after the growth of the crystals. Before trying to find an explanation for these features, we mention the bluish color of Sm doped samples of SrF_2, which is very similar to that of the same samples which had been subjected to reductive treatments like hydrogenation (see Hall and Schumacher[10]) or additive coloration (Den Hartog[11]). Samples of the latter type are colored very strongly, probably as a result of the reduction of Sm^{3+} to Sm^{2+}.

The bluish color has not been observed in the other rare-earth doped crystals of SrF_2. As the coloration of SrF_2:Sm was already present in the freshly grown boules, it is possible that the Sm^{3+}-F_i^- dipole complexes are accompanied by an extra divalent Sm^{2+} impurity. We suggest this to be the reason for the deviating behavior of SrF_2:Sm.

In going from La to Lu in $SrF_2:R$, one sees that

TABLE IV. ITC data for SrF_2:Sm. $N_d\Pi$ has been calculated from Eq. (2) with the strength of nn dipoles (0.65×10^{-28} Cm); Π has been calculated with Eq. (3).

Sample No.	Peak	t_p (sec)	T_p (K)	E_0 (eV)	p (eV)	τ_0 (sec)	$N_d\Pi$ (cm^{-3})	Π	T_m (K)
	b	1800	154.3	0.480	0.0027	8.7×10^{-14}	2×10^{17}	0.99	160.6
1	$a1$	900	151.5	0.417	0.0020	4.4×10^{-13}	82×10^{17}	1.00	146.7
	$a2$	1200	128.6	0.408	0.0021	7.1×10^{-13}	10×10^{17}	0.16	146.0
	$a3$	1800	140.8	0.409	0.0041	9.3×10^{-13}	69×10^{17}	0.99	147.3
2	$a4$	900	140.8	0.415	0.0063	4.3×10^{-13}	35×10^{17}	0.95	146.0
	$a5$	900	136.7	0.406	0.0058	8.0×10^{-13}	23×10^{17}	0.71	145.4

very slight changes in the nature of the impurity ion can give rise to a drastic change in the type of charge compensation that takes place. It is therefore plausible that a Sm^{2+} ion, situated at a Sr^{2+} lattice site next to the Sm^{3+} ion, makes nnn compensation more favorable than nn compensation. The existence of Sm^{+} impurities in SrF_2:Sm can be ruled out because with EPR, which is a very sensitive technique for the observation of Sm^{+} ($4f^7$ electron configuration), we have not been able to detect this type of impurity. The observed values of τ_0 for the depolarization process of peak *a* are significantly different from the ones that have been found for type-I and type-II reorientation.

The data obtained from the fitting of peak *b* have larger maximum errors than the other corresponding numbers in this paper because of the very low intensity of this peak. We estimate: $\Delta E_0 = 0.03$ eV and $\Delta \log_{10}\tau_0 = 1$. The uncertainty in T_m remains unaltered: $\Delta T_m = 1$ K.

In SrF_2:Eu an ITC band has been observed near $T_m \approx 150$ K. Depending on the polarization temperature T_p, T_m ranged from 150.4 to 152.5 K and the fitted relaxation parameters E_0 and τ_0 from 0.449 to 0.493 eV, and from 8.0×10^{-14} to 4.5×10^{-15} sec, respectively. In all cases p was found to be very large, as compared with the intensity of the band. These results confirm the experimental results of Wagner and Mascarenhas,[12] who reported a double peak near 150 K in SrF_2:Eu. They have been able to separate the components experimentally, but the values of E_0 and τ_0 are rather inaccurate: 0.28 $\pm$ 0.03 eV and 5×10^{-8} sec for the first, and 0.33 $\pm$ 0.03 eV and 3×10^{-9} sec for the second peak. In view of our ITC results of the series SrF_2:R^{3+} it remains to be seen whether the error bars as given by *W* and *M* are large enough. It is possible that the composite band in SrF_2:Eu is a superposition of two peaks similar to the ones that are observed in SrF_2:Sm. The similarity between Sm and Eu follows from the well-known phenomenon that Eu, too, has a tendency to be present in the divalent state. In contrast with Sm^{2+} the Eu^{2+} impurities do not give rise to blue colored crystals.

D. Interaction between different kinds of dipoles

In order to study the interaction between two different kinds of dipoles in one sample, we have examined a number of crystals SrF_2 simultaneously doped with La and Lu in varying concentrations. In these crystals both type-I and type-II dipoles are present. This is also the case in SrF_2:Gd, Tb, Dy. Equations (12) and (15) are applicable to the experimental results of these samples.

Although the values of the parameters presented in this paper are all based on computer fits with qualities varying between good and excellent, it is seen that the determination of p is relatively inaccurate (cf. Figs. 3 and 5). In order to achieve reliable estimates for the value of p_2/p_1 it is therefore necessary to consider the results from the excellent fits only. For these we estimate the maximum error in p to be 0.0010 eV. The experimental results have been compiled in Table V. It appears that, in spite of the high-quality requirements imposed on the computer fits, we still deal with large errors in the calculated values of p_2/p_1.

According to the theory, p_2/p_1 equals unity when elastic deformation effects are dominant, whereas $p_2/p_1 = \mu_2/\mu_1$ in case we only deal with electrostatic dipole-dipole interaction. Sherstkov *et al.*[13] have found from electric field effect experiments on SrF_2:Gd that $\mu_2/\mu_1 = 2.0 \pm 0.5$. Matthews and Crawford,[14] who studied the ratio of the concentrations of type-I and type-II dipoles in SrF_2:Gd as a function of polarization temperature, find $\mu_2/\mu_1 = 2.4$ to give the best agreement with their experimental data. In our laboratory electric-field-effect experiments are in progress in order to determine the effective dipole moments more accurately. Preliminary results[15] indicate that indeed the value of μ_2/μ_1 exceeds the UPIM value of $\sqrt{3}$.

From Table V it follows that $p_2/p_1 = 1.75 \pm 0.50$.

TABLE V. ITC data for SrF_2 samples containing different kinds of dipoles.

Sample No.	Dopant	E_0 (eV)	p (eV)	τ_0 (sec)	N_d (cm^{-3})	p_2/p_1
1	La	0.490	0.0037	8.4×10^{-15}	15×10^{17}	1.57 ± 0.70
	Lu	0.634	0.0058	2.0×10^{-14}	41×10^{17}	
2	La	0.474	0.0028	3.1×10^{-14}	9×10^{17}	1.93 ± 1.05
	Lu	0.631	0.0054	2.3×10^{-14}	55×10^{17}	
3	Tb	0.457	0.0042	2.0×10^{-14}	21×10^{17}	1.93 ± 0.70
		0.639	0.0081	3.7×10^{-14}	38×10^{17}	

As the theory predicts a value between 1 and μ_2/μ_1, we conclude, regarding the quoted experimental determinations of μ_2/μ_1, that both elastic lattice deformation and electrostatic interaction are responsible for a significant broadening of the ITC band.

IV. DISCUSSION

A. Relaxation parameters

For type-I dipoles in SrF_2:R^{3+} we have found for the characteristic relaxation time $-14.3 \leq \log_{10}\tau_0 \leq -13.3$ with no significant correlation between τ_0 and the radius of the R^{3+} ion. The type-II dipoles also lack this correlation, but have slightly longer relaxation times: $-13.7 \leq \log_{10}\tau_0 \leq -13.0$. Timans and Den Hartog[6] have performed ir-absorption experiments on R^{3+}-H_i^- dipole complexes in SrF_2. These dipoles are very similar to the R^{3+}-F_i^- complexes studied in this paper. The ir-technique allows one to determine the frequencies of the various vibrational modes of the dipole with an accuracy better than 0.5%. In this way Timans and Den Hartog have observed that the maximum variation in τ_0 in going from La to Dy (type-I dipoles) is 6%. Our (less accurate) ITC results are in agreement with this behavior. Lenting *et al.*,[4] in their paper on reorientation of dipoles in SrF_2:R, have calculated from Eq. (17) corrected activation energies starting from the assumption that τ_0 has a constant value. For type-II dipoles they apparently have chosen a wrong value of τ_0, but their results concerning type-I dipoles are seen to be confirmed by an analysis of the data with the extended ITC formula.

Provided that a reliable value of τ_0 is available, it therefore appears that the method of calculating E_0 from T_m by means of Eq. (17) leads to more accurate results than, for example, the use of an Arrhenius plot of the low-temperature side of the ITC band. We have shown before[5] that the slope of the straight line in such a plot depends rather strongly on the dipole concentration. The temperature of the maximum of the peak is not affected by changes in the dipole concentration.

It has been suggested by Lenting *et al.*[4] that reorientation of nnn dipoles takes place by means of a jump of the F_i^- ion to a neighboring nn position. As, in general, nn dipoles reorient at lower temperatures than nnn dipoles, the F_i^- ion is then able to rotate freely around the R^{3+} ion, so that the frozen in polarization can disappear completely. Recently, Matthews and Crawford[14] have given a detailed discussion of the dipole relaxation mechanism in SrF_2:Gd. They also presented experimental evidence for the correctness of the above mentioned model. It seems to be applicable to the whole range of rare earths in SrF_2, except for Sm and Eu. We have found that the ITC band near $T_m = 146$ K in SrF_2:Sm should be ascribed to reorientation of type-II dipoles.

The observed value of τ_0 is about ten times as large as it is for other type-II dipoles, which indicates that we are dealing with a different relaxation mechanism. The occurrence of a second very small peak near $T_m = 161$ K probably has to be explained in terms of this mechanism. For example, part of the jumping F_i^- ions may be trapped in some potential energy minimum different from an nnn site. The anomalous behavior of N_dII as a function of T_p and t_p (cf. Table IV) points at a more complicated reorientation mechanism, too.

B. Dipole-dipole interaction

The theoretically calculated values of m in $p = mN_d$ (cf. Sec. II B) are too small by factors of 5.6 and 2.7 for type-I and type-II dipoles, respectively, when the broadening obtained from the crude electrostatic interaction model is compared with the experimental results. For type-I dipoles a refinement of the model by including the saddle-point configuration, appears to give only a slight change in m. We feel that the crudeness of the model cannot account for the observed discrepancy alone. Also the presence of considerable amounts of monopoles can be ruled out. It has been found by several authors that the concentration of monopoles increases drastically at high R^{3+} concentrations. From EPR experiments on SrF_2:Gd we have found that in our samples the concentration of cubic Gd^{3+} impurities relative to the dipole concentrations is extremely small. As we have used for our ITC studies samples with R^{3+} concentrations which are similar to the EPR samples mentioned above, we may conclude that in general the broadening due to monopole-dipole interactions can be neglected.

Evidently, only interactions between dipolar defects should account for the broadening of the ITC bands. Electrostatic interaction cannot do so alone. Therefore we have to assume that there is a significant contribution to the broadening of the ITC band from elastic deformations induced by dipolar electric fields. It was shown in Sec. II B that this kind of interaction is indeed comparable in magnitude with electrostatic interaction. Moreover, the elastic contribution has been seen to be more dominant for smaller dipole strengths. This would explain why the agreement between theory and experiment is better in the case of type-II dipoles than it is for type-I dipoles.

In Sec. III D, too, we have shown that elastic effects are not negligible. A second check is offered

by a comparison of Eqs. (13) and (16) with the experimental data given in the captions of Figs. 3 and 5. Equation (13) (dominating electrostatic interaction) gives $\mu_2/\mu_1 = 1.3 \pm 0.3$ and Eq. (16) (dominating elastic effects) gives $\mu_2/\mu_1 = 1.8 \pm 0.5$. The error bars follow from estimated maximum deviations of 15% in m_1 and m_2. With regard to the previously quoted experimental determinations of μ_2/μ_1,[13,14] we conclude again that elastic lattice deformations cannot be neglected.

V. CONCLUSIONS

The usefulness of the extended ITC formula has been well established by the experimental results presented in this paper. We have found that τ_0 does not depend significantly on the nature of the rare-earth ion in R^{3+}-F_i^- dipole complexes, which agrees with the results of ir-absorption studies[6] on R^{3+}-H_i^- centers. There exists a slight dependence between the unperturbed activation energy E_0 and the radius of the R^{3+} ion. Probably, also the electronic polarizability of the R^{3+} ion influences E_0. The variations in E_0 are limited to a couple of hundredths of an electronvolt.

The drastic change in the type of charge compensation that is observed in going from Gd (dominant nn compensation) to Dy (dominant nnn compensation) indicates that the difference in the association energies for these types of charge compensation is also of the order of 0.01 eV. This explains why only a small change in the surroundings of a dipole, such as the presence of an additional Sm^{2+} ion located next to a Sm^{3+}-F_i^- complex, may give rise to dominant nnn compensation instead of the expected nn compensation.

The extra parameter p, introduced to account for dipole-dipole interaction, provides valuable information about the type of charge compensation (cf. SrF_2:Sm) and about the nature of the interaction effect. We have shown that electrostatic interaction between dipoles alone cannot explain the observed peak broadening; also contributions from elastic lattic deformation have to be considered. A tentative theoretical treatment of elastic perturbation effects appears to support this conclusion.

Lenting *et al.*[4] proposed that reorientation of nnn dipoles takes place via subsequent jumps of the F_i^- ion through nn sites. Independently, this relaxation mechanism has been proposed by Matthews and Crawford[14]; they also reported experimental evidence for its correctness. The observed features in SrF_2:R^{3+} are in agreement with this model, except for Sm and Eu, which show a deviating behavior.

ACKNOWLEDGMENTS

The authors are indebted to Dr. C. G. van der Laan of the Groningen University Computing Center for his contribution to the programming of the modified ITC formula. We are grateful to P. Wesseling for growing the crystals and to B. P. M. Lenting for recording a number of the ITC spectra. This work is part of the research programme of the "Stichting voor Fundamenteel Onderzoek der Materie" (FOM) and has been made possible by financial support from the "Nederlandse Organisatie voor Zuiver Wetenschappelijk Onderzoek" (ZWO).

[1] C. Bucci and R. Fieschi, Phys. Rev. Lett. 12, 16 (1964).
[2] E. L. Kitts Jr. and J. H. Crawford Jr., Phys. Rev. B 9, 5264 (1974).
[3] D. R. Stiefbold and R. A. Huggins, J. Solid State Chem. 5, 15 (1972).
[4] B. P. M. Lenting, J. A. J. Numan, E. J. Bijvank, and H. W. den Hartog, Phys. Rev. B 14, 1811 (1976).
[5] W. van Weperen, B. P. M. Lenting, E. J. Bijvank, and H. W. den Hartog, Phys. Rev. B 16, 2953 (1977).
[6] J. W. J. Timans and H. W. den Hartog, Phys. Status Solidi B 73, 283 (1976).
[7] *Handbook of Mathematical Functions*, edited by M. Abramowitz and I. A. Stegun (Dover, New York, 1965), p. 890.
[8] C. J. F. Böttcher, *Theory of Electric Polarization* (Elsevier, Amsterdam, 1973), p. 130.
[9] R. D. Shannon and C. T. Prewitt, Acta Crystallogr. B 25, 925 (1969).
[10] J. L. Hall and R. T. Schumacher, Phys. Rev. 127, 1892 (1962).
[11] H. W. den Hartog (private communication).
[12] J. Wagner and S. Mascarenhas, Phys. Rev. B 6, 4867 (1972).
[13] Yu. A. Sherstkov, V. A. Vazhenin, and K. M. Zolotareva, Sov. Phys. Solid State 16, 1352 (1975).
[14] G. E. Matthews Jr. and J. H. Crawford Jr., Phys. Rev. B 15, 55 (1977).
[15] A. Aalbers (private communication).